JOURNAL OF THERMOPHYSICS AND HEAT TRANSFER
Vol. 9, No. 1, January–March 1995

Cooling Panel Optimization for the Active Cooling System of a Hypersonic Aircraft

B. Youn* and A. F. Mills†
University of California, Los Angeles, Los Angeles, California 90024

Optimization of cooling panels for an active cooling system of a hypersonic aircraft is explored. The flow passages are of rectangular cross section with one wall heated. An analytical fin-type model for incompressible flow in smooth-wall rectangular ducts with coupled wall conduction is proposed. Based on this model, the minimum mass flow rate of coolant for a single cooling panel is obtained by satisfying hydrodynamic, thermal, and Mach number constraints. Also, the sensitivity of the optimal mass flow rate of coolant to each design variable is investigated. In addition, numerical solutions for constant property flow in rectangular ducts, with one side rib-roughened and coupled wall conduction, are obtained using a k-ε and wall function turbulence model, these results are compared with predictions of the analytical model.

Nomenclature

c_P = constant pressure specific heat
D_h = hydraulic diameter
F = objective function for optimization
f = friction factor, $(8\tau_w/\rho u_b^2)$
G_i = constraint function for optimization
H = height of duct
h_c = heat transfer coefficient, $[q_w/(T_w - T_b)]$
h_r = rib height
k = turbulence kinetic energy, thermal conductivity of fluid
k_s = thermal conductivity of duct wall
L_p = length of a single cooling panel
M = Mach number
$\dot{M}$ = total mass flow rate for a single cooling panel
Nu = Nusselt number, $(h_c D_h/k)$
N_x, N_y, N_z = number of grid points
P = pressure
Pr = laminar Prandtl number
p = rib pitch
q_w = wall heat flux
$\mathcal{R}$ = residual
Re = Reynolds number, $(u_b D_h/\nu)$
T = temperature
t_1 = thickness of bottom wall
t_2 = half-thickness of side wall
t_3 = thickness of top wall
u = velocity component in flow direction
W = width of rectangular duct
W_p = width of a single cooling panel
X_i = design variable for optimization
x, y, z = rectangular coordinates
ΔP = pressure drop
ε = dissipation rate of turbulence energy
ν = laminar kinematic viscosity
ρ = density
τ_w = wall shear stress
ϕ = dependent variables, P, u, T, k, ε

Subscripts
b = bulk
h = hydraulic
in = inlet
l = lower limit
opt = optimal
out = outlet
s = solid
u = upper limit
w = wall

Received Aug. 26, 1992; revision received Feb. 28, 1994; accepted for publication July 22, 1994.

*Graduate Research Engineer; currently Manager, Air-Conditioning/Refrigeration & Heating Appliance Division, Samsung Electronics, 416 Maetan-3dong Paldalgu, Suwon, Republic of Korea.

†Professor, Mechanical, Aerospace and Nuclear Engineering Department.

Introduction

DURING the past decade, a great deal of effort has been directed toward the development of reusable Earth-to-orbit hypersonic aircraft powered by air-breathing engines. In developing such an aircraft, thermal management is one of the key factors since intense heat is generated from the combustion of the fuel and by aerodynamic heating.

Most earlier work on thermal protection, e.g., Dukes et al.,[1] employed the cold structure concept in which heavy and costly heat shields are used to protect the inner structure. However, due to the apparent problems and restrictions of heat shields indicated by Becker,[2] the concept of active cooling has become more attractive. Helenbrook et al.[3] and Anthony et al.[4] have shown significant advantages of active cooling over the heat shield concept in weight and cost.

Usually the goal of aircraft structure design is to obtain a minimum weight, however, for hypersonic aircraft cooled by the hydrogen fuel the most crucial factor is the required coolant flow rate because of the limited fuel available. From a simple energy balance analysis it has been found that the required coolant flow rate exceeds the fuel flow rate for optimum engine performance at Mach numbers greater than about 10.[5]

Scotti et al.[6] used an optimization technique to find the minimum coolant flow rate subject to temperature, pressure drop, mechanical stress, thermal-fatigue-life, and Mach number constraints. They considered two types of cooling panel construction: 1) longitudinal fin (rectangular duct), and 2) pin-fin cooling jackets. The present work considered only hydrodynamic, thermal, and Mach number constraints, and smooth or rectangular rib-roughened duct geometry. The key objective of active cooling thermal analysis is to maintain the maximum surface temperature of the aircraft under the limit set by materials constraints (thermal constraint), and the out-

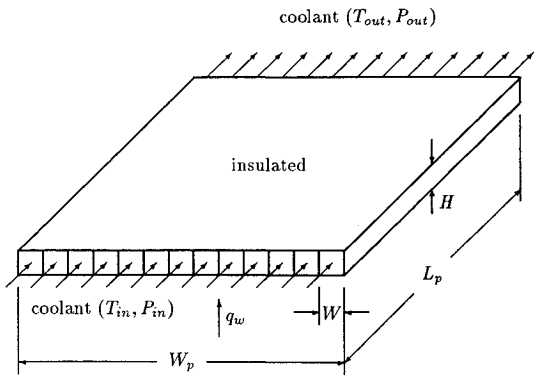

Fig. 1 Single cooling panel considered in the present work.

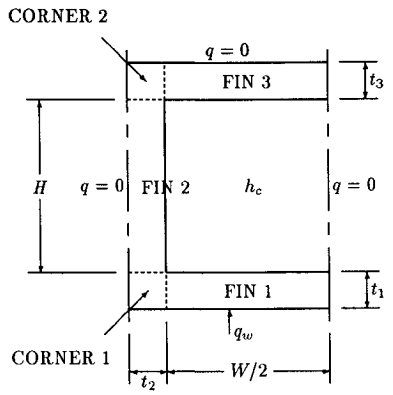

Fig. 2 Geometry of a single duct of the cooling panel.

let pressure of the hydrogen should be maintained above a limit value for proper fuel flow and penetration into the airstream in the scramjet engine[5] (hydrodynamic constraint). Also, a Mach number constraint for the coolant is required to avoid compressibility effects.

The present work considers a single cooling panel of width W_p and length L_p, shown in Fig. 1. It is assumed that the one side of cooling panel is exposed to a uniform q_w, and the other side is insulated, and also that there exists no axial diffusion, the thermophysical properties are constant and the flow is turbulent. First, an analytical model based on fin-type assumptions and existing correlations for friction and heat transfer for smooth walls is introduced. Based on this model, the numerical optimization software "CONMIN"[7] is used to obtain optimal parameters and investigate the sensitivity of optimal coolant mass flow rate to each design variable. Finally, the Navier-Stokes and energy equations governing incompressible flow in rectangular ducts with the heated side rib-roughened coupled to the heat conduction equation in the panel walls, are solved using the CFD package "PHOENICS."[8]

Analytical Model

Consider the rectangular duct geometry shown in Fig. 2. The model consists of 3 fins and 2 corners, and the convective heat transfer coefficient inside the duct is h_c. The bottom wall is exposed to a uniform q_w, and heat flux is zero at the left and right boundaries of the domain because of symmetry. An analytical model will be developed under the following assumptions:

1) There exists no temperature variation in the cross section of the duct walls (fin assumption).

2) There exists no temperature variation in the corners.

3) The convection coefficient h_c is constant everywhere (all walls are smooth).

4) Wall-conduction in axial direction is negligible.

5) The flow is fully developed.

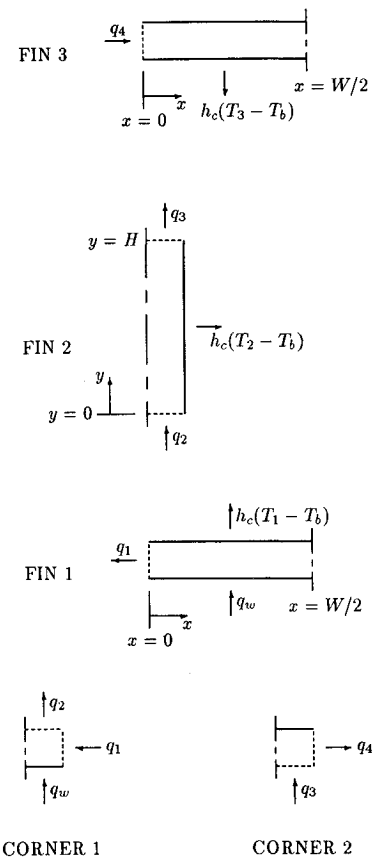

Fig. 3 Energy balance on fins and corners of rectangular duct.

The fins and corners are separated, and heat inputs and outputs are schematically shown in Fig. 3. From energy balances for fins 1, 2, and 3, we obtain the following ordinary differential equations, boundary conditions, and solutions (the coolant T_b is taken to be 0 for convenience):

Fin 1

Governing equation

$$\frac{d^2T_1}{dx^2} - \beta_1^2 T_1 = -\frac{\beta_1^2}{h_c} q_w, \qquad \beta_1 = \sqrt{(h_c/k_s t_1)} \tag{1}$$

Boundary conditions

$$k_s \left.\frac{dT_1}{dx}\right|_{x=0} = q_1 \tag{2}$$

$$k_s \left.\frac{dT_1}{dx}\right|_{x=W/2} = 0 \tag{3}$$

Solution

$$T_1 = -\frac{q_1 \cosh[\beta_1(W/2 - x)]}{\beta_1 k_s \sinh(\beta_1 W/2)} + \frac{q_w}{h_c} \tag{4}$$

Fin 2

Governing equation

$$\frac{d^2T_2}{dy^2} - \beta_2^2 T_2 = 0, \qquad \beta_2 = \sqrt{(h_c/k_s t_2)} \tag{5}$$

Boundary conditions

$$-k_s \left.\frac{dT_2}{dy}\right|_{y=0} = q_2 \tag{6}$$

$$-k_s \left.\frac{dT_2}{dy}\right|_{y=H} = q_3 \tag{7}$$

Solution

$$T_2 = \frac{q_2 \cosh[\beta_2(H - y)] - q_3 \cosh(\beta_2 y)}{\beta_2 k_s \sinh(\beta_2 H)} \tag{8}$$

Fin 3

Governing equation

$$\frac{d^2T_3}{dx^2} - \beta_3^2 T_3 = 0, \qquad \beta_3 = \sqrt{(h_c/k_s t_3)} \tag{9}$$

Boundary conditions

$$-k_s \left.\frac{dT_3}{dx}\right|_{x=0} = q_4 \tag{10}$$

$$k_s \left.\frac{dT_3}{dx}\right|_{x=W/2} = 0 \tag{11}$$

Solution

$$T_3 = \frac{q_4 \cosh[\beta_3(W/2 - x)]}{\beta_3 k_s \sinh(\beta_3 W/2)} \tag{12}$$

Applying energy balances to corners 1 and 2 we obtain the relations:

$$q_w t_2 + q_1 t_1 = q_2 t_2 \tag{13}$$

$$q_3 t_2 = q_4 t_3 \tag{14}$$

respectively, and additional relations can be obtained from the second assumption implying $T_1(x = 0) = T_2(y = 0)$, and $T_2(y = H) = T_3(x = 0)$. From these isothermal corner conditions the following relations are obtained:

$$-\frac{q_1 \cosh(\beta_1 W/2)}{\beta_1 k_s \sinh(\beta_1 W/2)} + \frac{q_w}{h_c} = \frac{q_2 \cosh(\beta_2 H) - q_3}{\beta_2 k_s \sinh(\beta_2 H)} \tag{15}$$

$$\frac{q_2 - q_3 \cosh(\beta_2 H)}{\beta_2 k_s \sinh(\beta_2 H)} = \frac{q_4 \cosh(\beta_3 W/2)}{\beta_3 k_s \sinh(\beta_3 W/2)} \tag{16}$$

Solving Eqs. (13–16) simultaneously for q_1, q_2, q_3, and q_4, we obtain

$$q_1 = \frac{A_2 B_3 - A_3 B_2}{A_2 B_1 - A_1 B_2} \tag{17}$$

$$q_2 = q_w + \frac{t_1}{t_2} q_1 \tag{18}$$

$$q_3 = \frac{A_3 B_1 - A_1 B_3}{A_2 B_1 - A_1 B_2} \tag{19}$$

$$q_4 = \frac{t_2}{t_3} q_3 \tag{20}$$

where

$$A_1 = \frac{1}{\beta_1 k_s} \coth(\beta_1 W/2) + \frac{t_1/t_2}{\beta_2 k_s} \coth(\beta_2 H)$$

$$A_2 = -\frac{1}{\beta_2 k_s \sinh(\beta_2 H)}$$

$$A_3 = \left[\frac{1}{h_c} - \frac{1}{\beta_2 k_s} \coth(\beta_2 H)\right] q_w$$

$$B_1 = \frac{t_1/t_2}{\beta_2 k_s \sinh(\beta_2 H)}$$

$$B_2 = -\frac{1}{\beta_2 k_s} \coth(\beta_2 H) - \frac{t_2/t_3}{\beta_3 k_s} \coth(\beta_3 W/2)$$

$$B_3 = -\frac{q_w}{\beta_2 k_s \sinh(\beta_2 H)}$$

Optimization

An optimization problem generally consists of an objective function $F(X_1, X_2, \ldots, X_n)$ to be minimized for design variables X_i for $i = 1, 2, \ldots, n$. The design variables may have lower $(X_{i,l})$ or upper $(X_{i,u})$ bounds (side constraints), and there can be a set of constraint functions such that

$$G_i(X_1, X_2, \ldots, X_n) < 0 \quad \text{for} \quad i = 1, 2, \ldots, m$$

The design variables for the present optimization problem are W, H, t_1, t_2, t_3, and u_b. The lower limits for duct dimensions taken by Scotti et al.[6] are $W_l = H_l = 0.4$ mm, and $t_{1,l} = t_{2,l} = t_{3,l} = 0.1$ mm. However, Wieting and Guy[5] considered offset-plate-fin heat exchangers with the dimensions of $H = 1.27$- and 0.15-mm fin thickness, and Hemmings and Purmort[9] used circular ducts of 3.6 mm i.d. and 0.25-mm wall thickness in their experiment. The present work takes $W_l = H_l = 2$ mm, and $t_{1,l} = t_{2,l} = t_{3,l} = 0.2$ mm, because the duct dimensions used by Scotti et al. are thought to be too small to manufacture.

Values for fixed parameters include a 1- × 1-m panel, $T_{in} = 50$ K, $P_{in} = 8$–34 MPa, and $q_w = 2$–20 MW/m^2 following Scotti et al. As mentioned previously, the objective function is coolant mass flow rate $\dot{M}$ for a single cooling panel that can be expressed in terms of the design variables, as

$$F = \dot{M} = \rho u_b W H \frac{W_p}{W + 2t_2} \tag{21}$$

P_{out} should be higher than a prescribed limit $P_{out,l}$ for a proper engine operation, and the first constraint (hydrodynamic constraint) function is

$$G_1 = \Delta P - P_{in} + P_{out,l} < 0 \tag{22}$$

ΔP can be calculated from existing correlations for the friction factor, for which the following correlation suggested by Kays and London[10] is used:

$$f = 0.184 Re^{-0.2} \tag{23}$$

Using this correlation, Eq. (22) can be rewritten in terms of the design variables as

$$G_1 = 0.04 \rho \nu^{0.2} u_b^{1.8} [(W + H)/WH]^{1.2} L_p - P_{in} + P_{out,l} \tag{24}$$

As mentioned previously, the duct wall temperature should be maintained under the material limit $T_{s,u}$. Intuitively we expect T_{max} to occur on the bottom wall (fin 1), however, it

Table 1 List of candidate materials for cooling panel and their properties

	Nickel 201	Zirconium copper	Titanium aluminide
$T_{s,u}$, K	1110	811	1030
k_s, W/mK	60.6	346	13.8

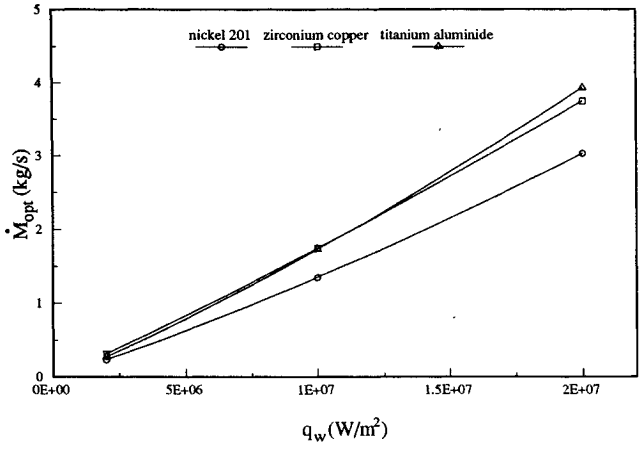

Fig. 4 Comparison of candidate materials for cooling panels.

can be located at either end of fin 1. Thus, the thermal constraint gives two constraint functions, G_2 and G_3

$$G_2 = T_1(x = 0) + T_{out} - T_{s,u} < 0 \quad (25)$$

$$G_3 = T_1(x = W/2) + T_{out} - T_{s,u} < 0 \quad (26)$$

Temperature T_1 is calculated using Eq. (4), where h_c is obtained from a modified Colburn analogy for internal turbulent flow

$$Nu = 0.023Re^{0.8}Pr^{0.4} \quad (27)$$

The coolant T_{out} is calculated from an overall energy balance on the panel

$$T_{out} = \frac{q_w(W + 2t_2)L_p}{\rho c_p u_b WH} + T_{in} \quad (28)$$

A Mach number constraint for the coolant is required to avoid compressibility effects. The estimated speed of sound for hydrogen fuel is about 1000 m/s, and a Mach number limit $M_u = 0.25$ was used by Scotti et al.[6] This condition can be satisfied simply by limiting u_b less than 250 m/s, and no constraint function is required.

Scotti et al. considered three candidate materials, nickel 201, zirconium copper, and titanium aluminide (properties of these materials are listed in Table 1). The optimal coolant flow rate for each material was obtained using the present model and constraints, and typical results are shown in Fig. 4. Nickel 201 gives the lowest optimal flow rates and, thus, only nickel 201 was considered for further study.

All the parameters for the optimization, such as design variables and fixed parameters, and their ranges are listed in Table 2, and the software CONMIN[7] was used for the optimization.

Optimization Results

Figure 5 shows the variation of $\dot{M}_{opt}$ as a function of q_w. The results for P_{in} = 8, 20, 34 MPa fall on one curve, which implies that the pressure drop constraint does not have any influence. It was found that $\dot{M}_{opt}$ occurs at the minimum values

Table 2 List of parameters involved in the optimization

Design variables	Fixed parameters	Properties
W, 2 mm	W_p, 1 m	ρ, 50 kg/m^3
H, 2 mm	L_p, 1 m	ν, 2 × 10^{-7} m^2/s
t_1, 0.2 mm	T_{in}, 50 K	k, 0.1 W/mK
t_2, 0.2 mm	P_{in}, 8–34 MPa	c_p, 10,000 J/kgK
t_3, 0.2 mm	q_w, 2–20 MW/m^2	Pr, 1.0
u_b, 0–250 m/s	$P_{out,b}$, 5 MPa	a, 1,000 m/s
		k_s, 60.6 W/mK
		$T_{s,u}$, 1,110 K

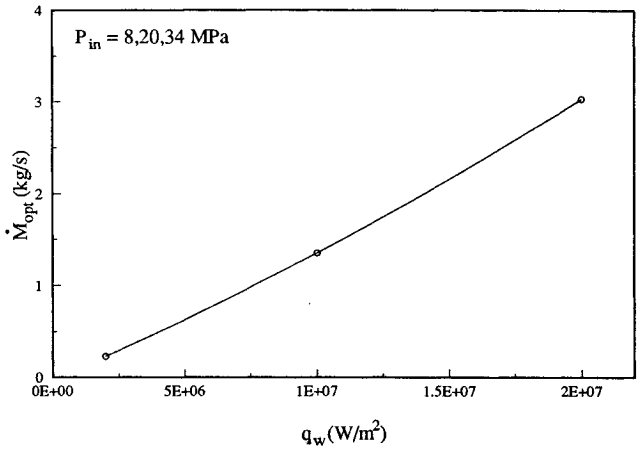

Fig. 5 Variation of $\dot{M}_{opt}$ as a function of q_w (W_l = H_l = 2 mm).

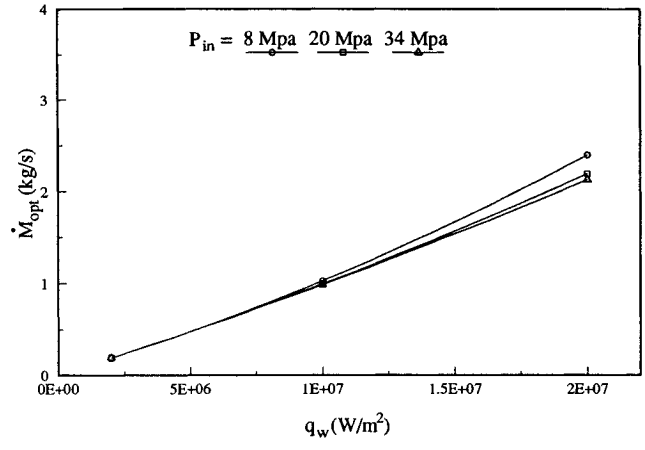

Fig. 6 Variation of $\dot{M}_{opt}$ as a function of q_w (W_l = H_l = 0.2 mm).

of W and H when the ΔP constraint has no effect, thus, if the lower bounds W_l and H_l are relatively large (2 mm), the ΔP constraint does not come into play. The pressure drop is less than 1 MPa in all the cases, which means that the ΔP constraint is always satisfied, provided P_{in} is higher than 6 MPa. In the present optimization W_{opt} and H_{opt} are identically equal to W_l (2 mm) and H_l (2 mm), respectively. On the contrary, when W_l and H_l are relatively small, the ΔP constraint comes into play. Figure 6 shows the variation of $\dot{M}_{opt}$ as a function of q_w for W_l = H_l = 0.2 mm. By decreasing the allowable duct size, $\dot{M}_{opt}$ has been reduced as much as 20–30%, and the ΔP constraint has an influence at high q_w and low P_{in}. When q_w is high, the required mass flow rate and resultant pressure drop increase, and then W and H need to be increased to satisfy the ΔP constraint, despite a penalty in heat transfer efficiency.

The total number of longitudinal fins (fin 2) in Fig. 3 for a single cooling panel is a crucial factor in determining overall performance of the panel as a heat exchanger. As more fins

are installed, the heat transfer efficiency increases, but more pumping power is required. In Fig. 7, as W increases, the number of fins per unit width of the cooling panel decreases, and the overall performance is degraded. In Fig. 8, the overall performance is degraded as H is increased, because the fin efficiency decreases as the fin length increases.

As discussed above, the pressure drop constraint does not play any role in the optimization for the range of parameters considered here. Also, it has been found that u_b is less than 100 m/s for all cases. Thus, hydrodynamic and Mach number constraints can be put aside.

It is beneficial to know the sensitivity of $\dot{M}_{opt}$ to each design variable. By analyzing the sensitivity of the objective function to each design variable we can reduce the number of variables

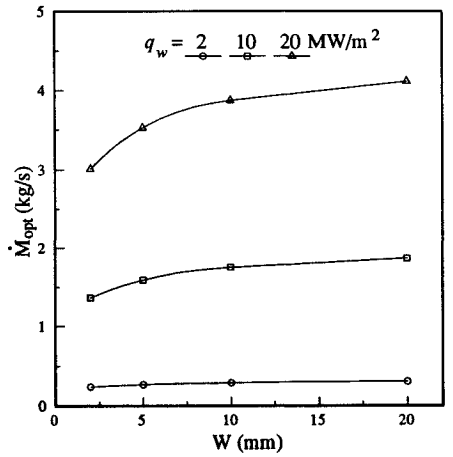

Fig. 7 Sensitivity of $\dot{M}_{opt}$ to W ($t_1 = t_3 = 0.2$ mm).

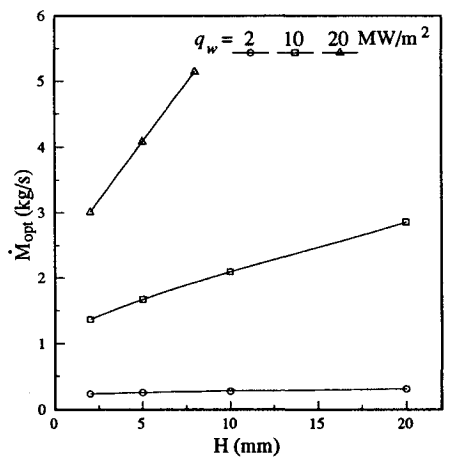

Fig. 8 Sensitivity of $\dot{M}_{opt}$ to H ($t_1 = t_3 = 0.2$ mm).

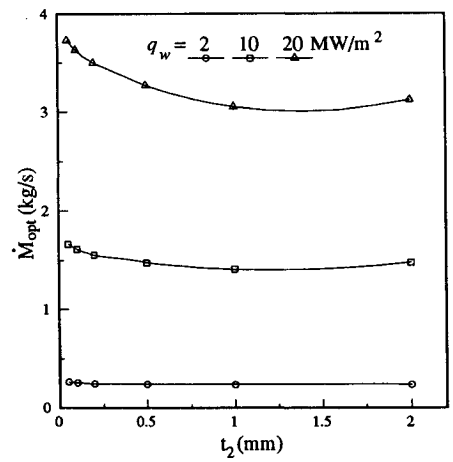

Fig. 9 Sensitivity of $\dot{M}_{opt}$ to t_2 ($t_1 = t_3 = 0.2$ mm).

to be considered in the full-scale computation. Figures 7 and 8 show the sensitivity of $\dot{M}_{opt}$ to W and H, respectively. As discussed above, $\dot{M}_{opt}$ monotonically increases as W and H increase, because the pressure drop constraint has no effect. If the ΔP constraint had an effect, there could be infeasible ranges for W and H, but for the current range of parameters this does not occur.

It was found that t_2 has a significant effect on $\dot{M}_{opt}$, as shown in Fig. 9, whereas t_1 and t_3 have negligible effects. As the thickness of fin 2 increases, the fin efficiency improves and, thus, $\dot{M}_{opt}$ decreases. However, if fin 2 is too thick, the total number of such fins for a single cooling panel is reduced, and this effect offsets the improved fin efficiency. Thus, $\dot{M}_{opt}$ first decreases with increasing t_2, but then the trend is reversed. Notice also that too large a value of t_2 invalidates the one-dimensional fin assumption.

Computational Results

Based on the above optimization results, governing equations for incompressible turbulent flow in rectangular ducts with the bottom wall rib-roughened (shown in Fig. 10) were numerically solved using the CFD package PHOENICS.[8] The k-ε turbulence model, and wall functions for rough surfaces from Webb et al.,[11] were utilized. Two-dimensional coupled wall conduction was included, although the existence of the fins was ignored for this purpose. The following duct dimensions were taken as base case values: $W = 2$ mm, $H = 2$ mm, $t_1 = 0.2$ mm, $t_2 = 0.4$ mm, $t_3 = 0.2$ mm; roughness element $h_r/D_h = 0.04$, $p/h_r = 10$. Unless otherwise stated, the above dimensions have been used. Details of the governing equations, turbulence model, and computational method may be found in our previous publications.[12-14]

The numerical scheme used in PHOENICS is first-order-accurate as a whole. In the present work, a conventional convergence criterion is applied

$$\left| \frac{\phi^i - \phi^{i-1}}{\phi^i} \right| < 10^{-4} \tag{29}$$

where the superscript is the iteration counter. This type of convergence criterion may lead to unconverged solutions when the convergence rate is extremely slow because of nonlinearity or under-relaxation, and thus the residuals for the governing equations need to be checked. (The residual is the sum of imbalances between the left and right sides of the discretized equations for each grid point.) A comparison of the residuals and the total convection rate $\int \rho u \phi \, dA$ for a typical case is made in Table 3. The order of the normalized residuals ranges between 10^{-4}–10^{-8}, and thus the choice of convergence criterion in the present work is considered to be appropriate. Also, a grid convergence test was performed to ensure convergence of solution as the grid size is refined, and to determine proper grid size. An exponential grid scheme is used in

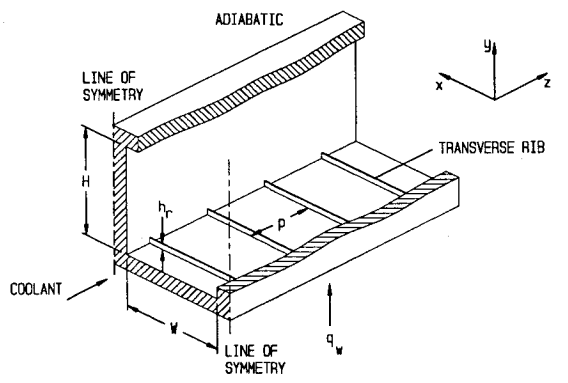

Fig. 10 Geometry of a single duct of a cooling panel with one side rib-roughened.

Table 3 Comparison of residuals and convection rate for a typical case

Governing equation	$\mathcal{R}$	$\int \rho u \phi \, dA$	$\mathcal{R}/\int \rho u \phi \, dA$
Mass	9.35×10^{-9}	0.393	2.38×10^{-8}
z momentum	5.45×10^{-6}	39.7	1.37×10^{-7}
Energy	4.99×10^{-2}	2.35×10^{5}	1.37×10^{-7}
k	8.81×10^{-5}	10.1	8.72×10^{-6}
ε	11.8	7.65×10^{4}	1.54×10^{-4}

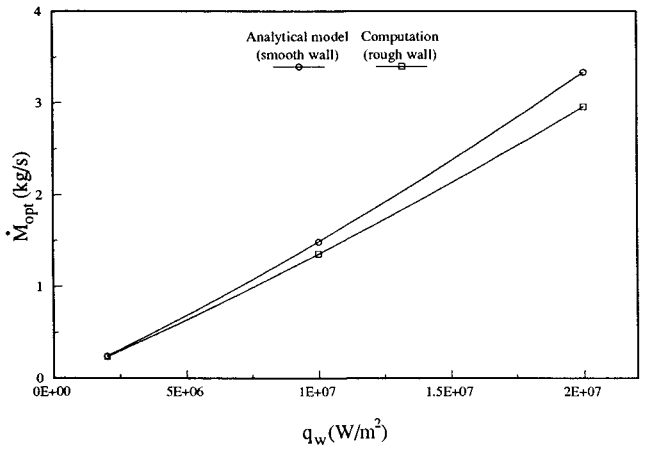

Fig. 11 Comparison of $\dot{M}_{opt}$ between the analytical model and numerical computation.

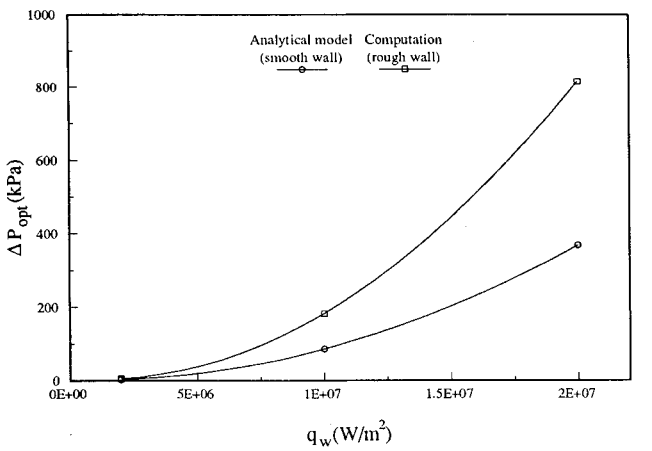

Fig. 12 Comparison of ΔP_{opt} between the analytical model and numerical computations.

x and y directions, and number of grids used in the present work is $33(N_x) \times 53(N_y) \times 300(N_z)$.

Figures 11 and 12 show the comparisons of $\dot{M}_{opt}$ and ΔP_{opt}, respectively, between the analytical model and the numerical computations. The optimal flow rate for the numerical results was determined as follows:

1) Geometric parameters were set equal to the base case values.

2) Several cases with varying u_b were run, and T_{max} data were assessed.

3) Interpolation was used to find the value of $\dot{M}$ that corresponds to $T_{max} = T_{s,a}$; the $\dot{M}$ thus obtained is $\dot{M}_{opt}$.

By adding rib roughness to the heated wall, $\dot{M}_{opt}$ is reduced by about 10%, and ΔP_{opt} increases by about 100%. Even though the pressure drop is considerably increased, it is still less than 1 MPa and, thus, the pressure drop constraint does not play a role. Considering that entrance effects have not been taken into account in the analytical model, ΔP_{opt} values will be a little higher in practice.

Since at least 10 numerical runs are needed to determine $\dot{M}_{opt}$ for each case, T_{max} was used instead of $\dot{M}_{opt}$ to investigate the effect of each design variable. T_{max} is the maximum cooling panel temperature that occurs on the heated wall at the coolant exit. Figure 13 shows the variation of T_{max} as a function of W. The trends shown by the numerical results are very similar to the predictions by the analytical model—T_{max} increases as W increases, whereas ΔP decreases due to the reasons discussed previously.

The effect of H on T_{max} is shown in Fig. 14. T_{max} generally increases as H increases, due to the degraded fin efficiency as stated previously. The numerical results are more sensitive than the analytical model to the variation of H, and T_{max} is even higher for the rough wall than for the smooth wall, for $H = 5$ mm. If this were true, there would be no gain in panel performance by introducing ribs, but only a penalty in pressure drop. However, the analytical model assumes h_c = const around the periphery of the channel. The definition of heat transfer coefficient based on fluid bulk temperature presents a dilemma as the channel aspect ratio increases. The numerical results show that the wall temperature is lower than the fluid bulk temperature for the upper part of the side wall and the entire upper wall. On the contrary, for the analytical model it is implied that the wall temperature is always higher than the bulk temperature. Thus, the analytical model underestimates T_{max} and $\dot{M}_{opt}$.

Figure 15 shows the variation of T_{max} as a function of t_2. As t_2 increases, T_{max} reaches its minimum earlier and increases more rapidly for the numerical results than for the analytical model. The adverse effect of too great an increase in t_2 has

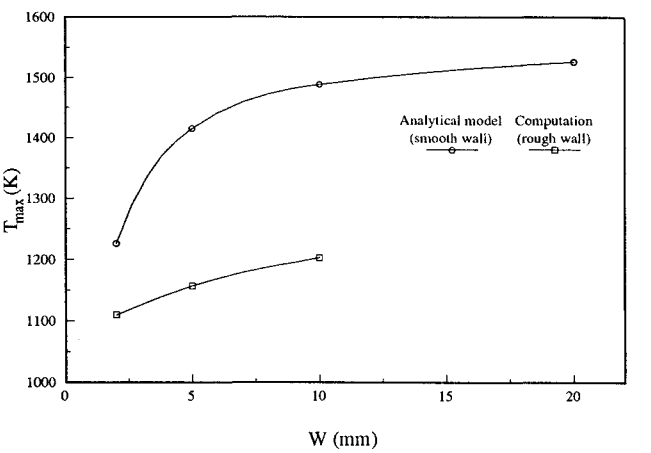

Fig. 13 Variation of T_{max} as a function of W ($\dot{M}$ = 2.975 kg/s, q_w = 20 MW/m^2).

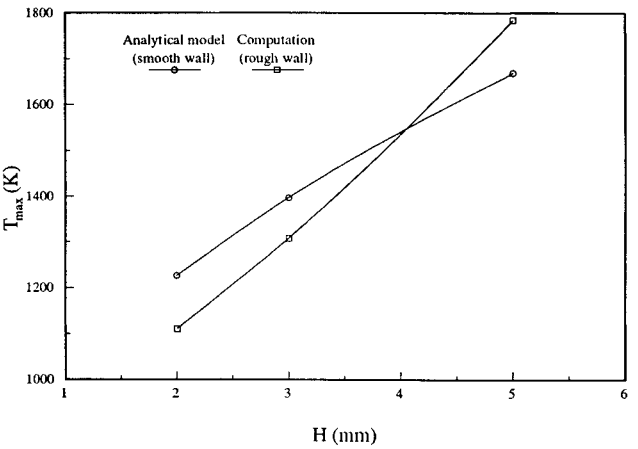

Fig. 14 Variation of T_{max} as a function of H ($\dot{M}$ = 2.975 kg/s, q_w = 20 MW/m^2).

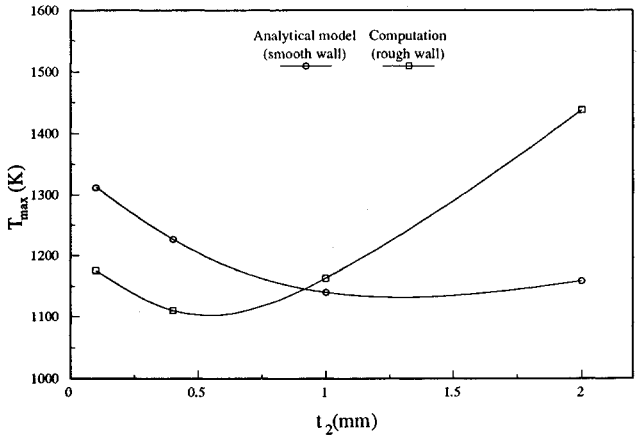

Fig. 15 Variation of T_{max} as a function of t_2 ($\dot{M}$ = 2.975 kg/s, q_w = 20 MW/m²).

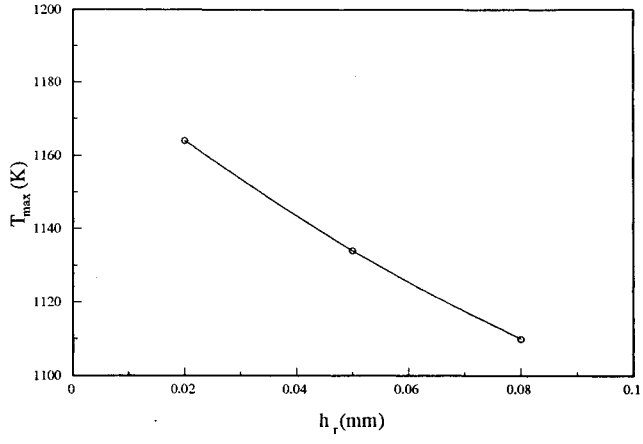

Fig. 16 Variation of T_{max} as a function of h_r (computation, $\dot{M}$ = 2.975 kg/s, q_w = 20 MW/m², p = 0.8 mm).

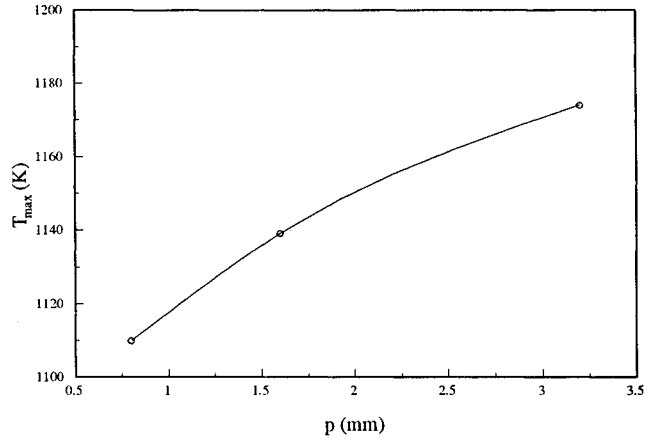

Fig. 17 Variation of T_{max} as a function of p (computation, $\dot{M}$ = 2.975 kg/s, q_w = 20 MW/m², h_r = 0.08 mm).

been already discussed for the analytical model, and it is more severe for the numerical results, since there exists a temperature variation in transverse direction for fin 2 when it is thick. Thus, as a fin is thickened, the fin efficiency is not improved as much as indicated by the fin analysis. Most of the design variables have opposing effects on T_{max} and ΔP, that is to say, if there is a gain in thermal efficiency, a penalty in pumping power is expected. However, in case of t_2, penalties in both thermal efficiency and pumping power are found for $t_2 > t_{2,opt}$.

Figures 16 and 17 show the effect of roughness size, h_r, and p, respectively. T_{max} becomes lower and ΔP becomes higher as the roughness element height increases and pitch is reduced. Notice that in Fig. 17, $p/h_r > 10$ and, thus, the heat transfer coefficient decreases with increasing p/h_r[11]; the observed increase in T_{max} results.

Summary

An analytical model for incompressible flow in rectangular ducts with coupled heat conduction based on fintype assumptions was developed. An optimization technique was applied to this model to find the minimum mass flow rate for a single cooling panel of 1 × 1 m (nickel 201), accounting for thermal, hydrodynamic, and Mach number constraints.

Based on the optimization results, full-scale computations were done with roughness added to the heated wall using the PHOENICS CFD package, and comparisons were made. An important result was that the individual duct size should be as small as possible, provided that the pressure drop constraint is met. For the range of parameters considered, the pressure drop for 1 m length of cooling panel is less than 1 MPa and, thus, is not a critical issue. It was also found that the side wall thickness is one of the key factors controlling the heat transfer efficiency of a cooling panel. As this thickness increases, $\dot{M}_{opt}$ decreases because of improved fin efficiency, however, this trend is reversed at a certain point because the total number of the fins for a single cooling panel are reduced when each fin is too thick. In reality, the fin efficiency does not increase as much as predicted by the analytical model because of temperature variation in transverse direction as t_2 increases. Inappropriate selection of side wall thickness results in penalties in both heat transfer efficiency and pressure drop.

It was also found that the analytical model underestimates $\dot{M}_{opt}$ because it assumes h_c = const with h_c defined in terms of the coolant bulk temperature. However, the numerical results showed that for a portion of the duct, the wall temperature is below the bulk temperature, and hence, the conventional definition of h_c is not applicable. Therefore, the heat transfer coefficient needs to be redefined for this type of problem, and appropriate correlations should be derived based on this new definition of h_c.

Acknowledgments

This work was funded by NASA Ames-Dryden Flight Research Facility through the UCLA Laboratory for Flight Systems, A. V. Balakrishnan, Director. The NASA Technical Officer was R. D. Quinn, and the funding was facilitated by K. Illif of NASA Dryden.

References

[1]Dukes, W. H., Gosden, C. E., Kappelt, G. F., and Mirti, A. E., "Manufacturing Methods for Insulated and Cooled Double-Wall Structures," Aeronautical Systems Div., Bell Aerospace Co., TR 61-7-799, Vols. I and II, Buffalo, NY, 1961.

[2]Becker, J. V., "New Approaches to Hypersonic Aircraft," The Seventh Congress of the International Council of the Aeronautical Sciences, Rome, Italy, ICAS Paper 70-16, Sept. 1970.

[3]Helenbrook, R. G., and Anthony, F. M., "Design of a Convective Cooling System for a Mach 6 Hypersonic Transport Airframe," NASA CR-1918, Dec. 1971.

[4]Anthony, F. M., Dukes, W. H., and Helenbrook, R. G., "Internal Convective Cooling Systems for Hypersonic Aircraft," NASA CR-2480, Feb. 1975.

[5]Wieting, A. R., and Guy, R. W., "Thermal-Structural Design/Analysis of an Airframe-Integrated Hydrogen-Cooled Scramjet," *Journal of Aircraft*, Vol. 13, No. 3, 1976, pp. 192–197.

[6]Scotti, S. J., Martin, C. J., and Lucas, S. H., "Active Cooling Design for Scramjet Engines Using Optimization Methods," NASA TM-100581, March 1988.

[7]Vanderplaats, G. N., "CONMIN—A Fortran Program for Constrained Function Minimization: User's Manual," NASA TM X-62,282,

Aug. 1973.

[8]PHOENICS (Parabolic, Hyperbolic Or Elliptic Numerical Integration Code Series), CHAM Ltd., London.

[9]Hemmings, B. R., and Purmort, W. P., "Actively Cooled Primary Structures, Optional Task 3," 5th Quarterly Review, Rocketdyne Div., Rockwell International Corp., 88RC04241, 1988.

[10]Kays, W. M., and London, A. L., *Compact Heat Exchangers*, 2nd ed., McGraw-Hill, New York, 1965.

[11]Webb, R. L., Eckert, E. R. G., and Goldstein, R. J., "Heat Transfer and Friction in Tubes with Repeated-Rib Roughness," *International Journal of Heat and Mass Transfer*, Vol. 14, 1971, pp. 601–618.

[12]Youn, B., "Flow of Supercritical Hydrogen in Rectangular Ducts," Ph.D. Dissertation, Univ. of California, Los Angeles, Los Angeles, CA, March 1991.

[13]Youn, B., and Mills, A. F., "Variable Property Flow in Rectangular Ducts with Repeated Rectangular Rib Roughness," *Phoenics Journal of Computational Fluid Dynamics and Its Applications*, Vol. 5, No. 2, 1992, pp. 175–232.

[14]Youn, B., and Mills, A. F., "Flow of Supercritical Hydrogen in a Uniformly Heated Circular Tube," *Numerical Heat Transfer, Part A: Applications*, Vol. 24, No. 1, 1993, pp. 1–24.